APPLICATION OF A HIGH POWER RUBY LASER BEAM FOR STUDYING PROPAGATION PHENOMENA OF LIGHT IN VARIOUS DIELECTRIC MEDIA

By F. Kaczmarek

Department of Molecular Physics, A. Mickiewicz University, Poznań*

A ruby laser with kryptocyanine "Q" switching cell operating in various resonator arrangements was investigated. Light pulses, single or in packets, were obtained ranging in duration from nsec to μsec, and depending on the pumping energy and Q factor of the laser optical cavity. The beam was then applied for studying propagation phenomena occurring at the surface or inside dielectric media. Due to molecular orientation and electrostriction, narrowing of the light beam in some substances was observed. At high power level of the light beam, photo-ionization of liquids and plasma generation at the glass-liquid interface of the cell have been observed.

1. Introduction

Nonlinear propagation of laser beams in liquids associated with ionization of the substance was previously described by this author in two short notes (1966). This paper contains some new results and a discussion on the influence of optical orientation and of electrostriction on the phenomena observed. To study propagation phenomena, a ruby laser provided with a kryptocyanine "Q" switching cell was built. Operation of this laser was investigated in detail; it was found to emit single light pulses as well as packets of pulses, depending on the pumping energy and optical quality of the resonator. Generation of plasma at the solid-liquid interface frequently observed during the course of experiments indicates that the threshold for breakdown caused by the electric field of the light wave is relatively low at the interface.

2. Apparatus

The laser device used in these experiments was described by this author in an earlier paper (1966). The energy of the laser beam (for a ruby rod of $l = 69.5$ mm and $\Phi = 7$ mm) as a function of the pumping energy is plotted in Fig. 1. Helical flashtubes were made of

---

* Address: Katedra Fizyki Molekularnej, Uniwersytet im. A. Mickiewicza, Poznań, ul. Grunwaldzka 6, Polska.

quartz and filled with spectroscopically pure xenon to a relatively high pressure ranging from 300 to 400 mm Hg. At an intermediate pumping energy level of 2500 J the rise time of the flash pulse was 50 μsec; the time was measured when a condenser bank of 277 μF
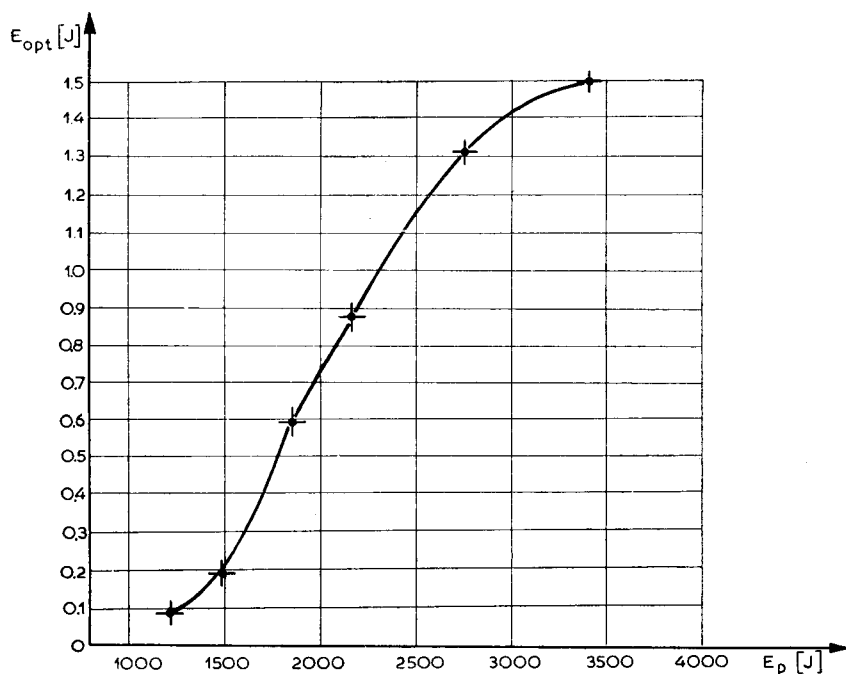

Fig. 1. Output energy of the ruby laser as function of pumping energy

was discharged through the tube connected in series with an air inductance coil of some 50 mH.

3. Measurements of pulse energy and its duration

The radiation energy of the laser beam was measured using the bolometer bridge proposed by Baker (1963). The measuring procedure and the bridge built in our laboratory have been described in detail by this author and co-workers (1967). The laser pulse duration was determined by means of a photodiode (Fig. 2) or photomultiplier (Fig. 3) monitoring device. The light detectors were connected through a distributed amplifier (operating in the frequency region form 5 kHz to 250 MHz) to an OSA type 601 wide band oscilloscope. Start of the time base was delayed by a simple thyratron circuit (Fig. 4) enabling continuous control of the time base start with respect to the moment of the flash tube discharge. This circuit was triggered by a signal from the flash tube triggering apparatus. In order to eliminate completely fluorescence from the ruby, the light from the flash tube, and the disturbing electromagnetic signals generated during battery discharge, light monitor devices were situated at some distance from the laser head. The distance varied from several
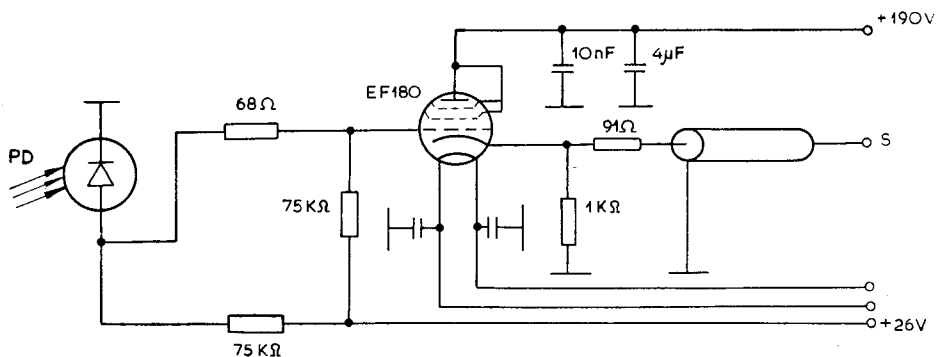
Fig. 2. Photodiode laser beam detector and CF preamplifier
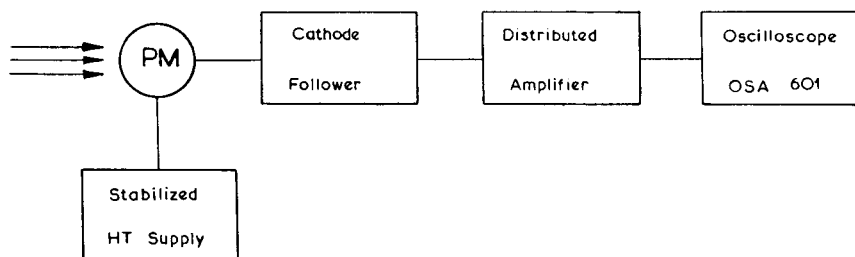
Fig. 3. Photomultiplier detector and the electronic circuit for monitoring of laser spikes
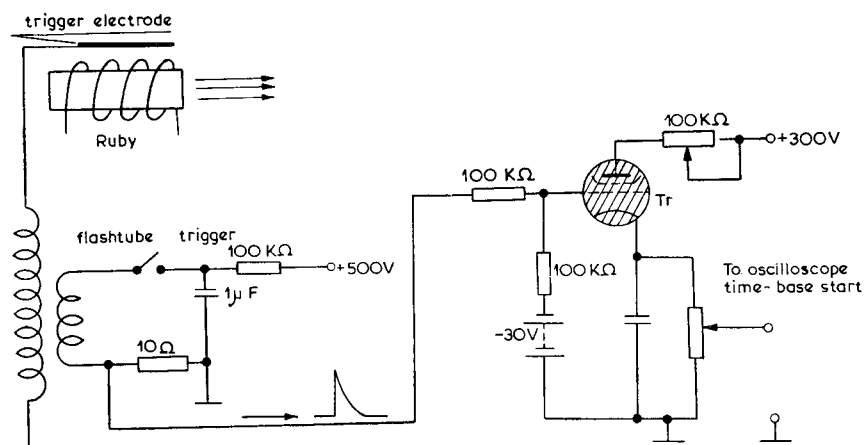
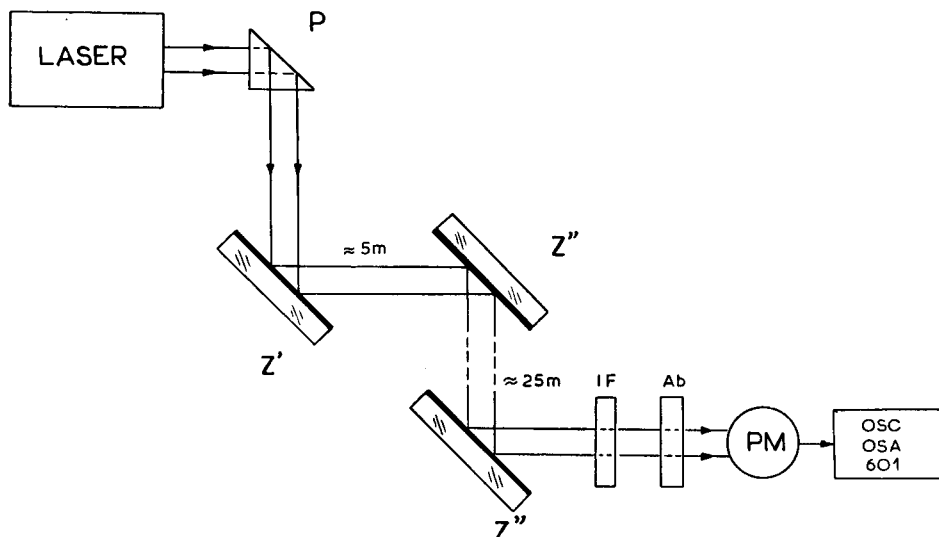Fig. 4. Device for time-delay of the oscilloscope time base start

Fig. 5. Scheme of the light beam directors used for separation of the laser device from the monitoring arrangement

up to about 30 m. In the last case the monitoring device and laser were placed in different laboratory rooms and the light beam from the laser was directed to the detector using mirrors and a prism (Fig. 5).

4. Investigation of laser spiking using a kryptocyanine Q switching liquid cell

The kryptocyanine Q switching cell is very often used in giant pulse operation of a ruby laser. The optical quality of the resonator is decreased by placing within this resonator a glass cell filled with kryptocyanine dissolved in methanol. Kryptocyanine exibits sharp absorption at the laser wavelength, *i. e.* at 6943 Å. Thus, the population inversion required for
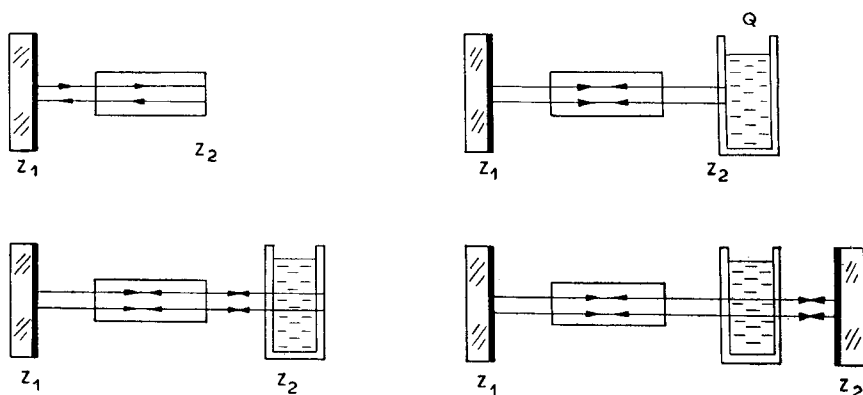

Fig. 6. Various possible ruby laser resonators used in the course of experiments
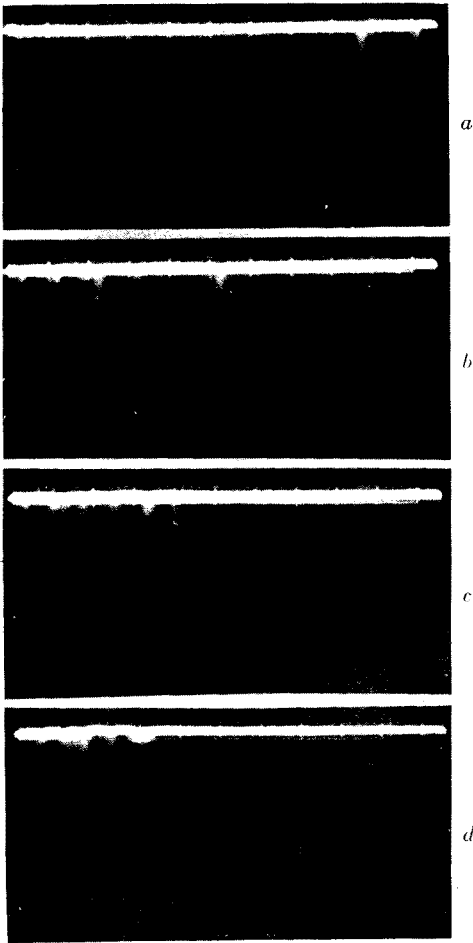
Fig. 7. Illustration of laser spiking with a krypto-cyanine Q switching cell and both dielectric mirrors in place. Transmission coefficient of this cell measured at the ruby laser wave-length was some 40%. Time base = 50 μsec/div. a) Pumping energy, $E_p = 1560$ J, b) $E_p = 1755$ J, c) $E_p = 1974$ J, d) $E_p = 2176$ J
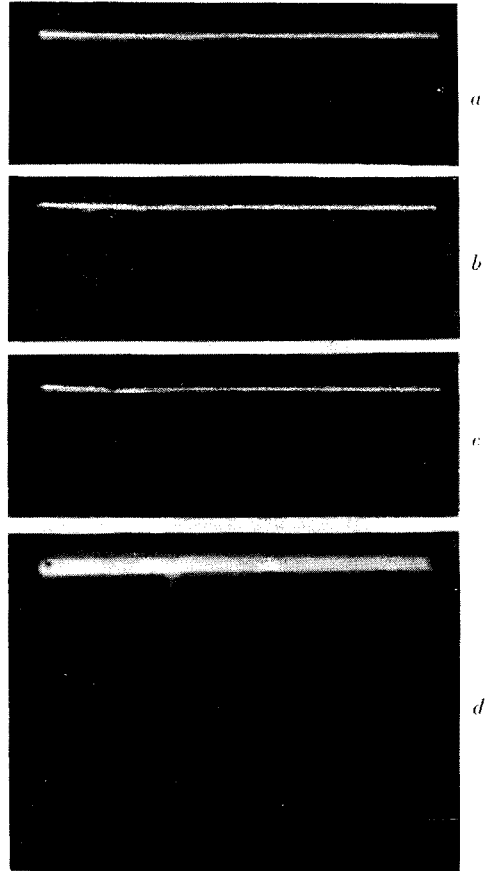
Fig. 8. Laser spike obtained using a kryptocyanine cell of transmittivity of 27%. Time base = 50 μsec/div. a) $E_p = 1850$ J, without output mirror b) $E_p = 2280$ J, as in a), c) $E_p = 2970$ J, as in a), d) $E_p = 2176$ J, both mirrors in place

Fig. 9. Single laser spike obtained using a kryptocyanine cell of transmittivity of 7.5%. Time base — 50 μsec/div. a) $E_p = 3260$ J, without output mirror, b), c) and d) — laser spike display at constant pumping energy of 3180 J with both mirrors in place. A decrease of the succesive laser spike can bee seen
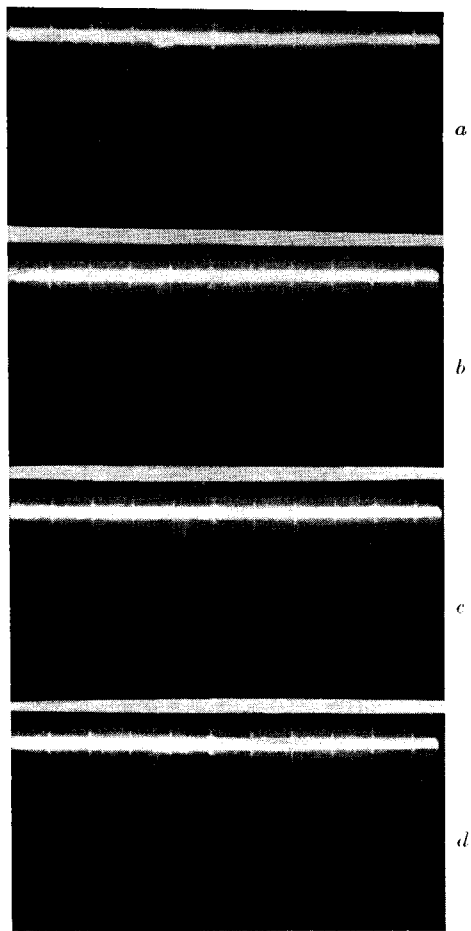
laser operation in ruby is increased and the laser could be optically pumped to higher energy regions. Laser spiking can be generated in one of the following optical resonators (Fig. 6):

1. Total reflection mirror Z_1, flat polished terminal of the ruby rod (serving as second mirror),

2. Mirror Z_1, ruby face and front wall of the liquid cell,

3. Mirror Z_1, output mirror Z_2 (kryptocyanine cell within the resonator).

All these arrangements form optical resonators of different Q factors and, of course, require various pumping energy thresholds for laser operation. The reflection coefficient of the ruby face for perpendicular incidence is relatively high (8%) and that of the glass wall of the cell is lower (4%). Radiation energy loss in the ruby rod were analyzed by Godwin (1965) and are caused by impurities (10^{-8} up to 10^{-6} cm^{-1}), scattering of light (3.10^{-3} up to 6.10^{-3} cm^{-1}), optical inhomogeneities (10^{-2} up to 10^{-1} cm^{-1}), and by diffraction. Diffraction loss could be neglected for commonly used ruby rods having diameters of several mm. However, it has often been found that for some ruby resonators the light beam was much narrower than the ruby diameter, and moreover light channels of high flux densities were created. For such small light channels diffraction loss must be taken into account.

The optical quality of the resonator with a given ruby rod depends only on the reflection coefficient of the mirrors and on the transmission of the kryptocyanine cell. The Q factor of the cavity is defined as

$$Q = 2\pi\nu \frac{E}{P}, \tag{4.1}$$

where E denotes the energy stored within the resonator, and P — the dissipated power.

Total power dissipation in the resonator during one full cycle of a given light ray is (no liquid cell in place)

$$P(1-r_1)+P(1-r_2)\,r_1,$$

where r_1 and r_2 are reflection coefficients of the mirrors. Neglecting increase in light path in the ruby rod and assumming the total length of the resonator to be L we have $t = 2L/c$, where t denotes the time period of the resonator. Equation (4.1) takes the form

$$Q = 2\pi\nu \frac{P\dfrac{2L}{c}}{P(1-r_1r_2)} = \frac{4\pi L}{\lambda} \frac{1}{1-r_1r_2}. \tag{4.2}$$

If furthermore a kryptocyanine cell of transmittivity T is placed within the resonator, total energy dissipation per one full cycle can be written as $P(1-r_1r_2T^2)$. In this case

$$Q = \frac{4\pi L}{\lambda} \frac{1}{1-r_1r_2T^2}. \tag{4.3}$$

Table I presents Q values calculated for various transmission coefficients of the liquid cell. Reflection coefficients of the mirrors were unchanged: $r_1 = 0.99$, $r_2 = 0.50$. The calculated values indicate clearly that the Q factors are almost the same at the following optical arrangements: mirror Z_1 — flat surface of the ruby, mirror Z_1 — output mirror Z_2 and kryptocyanine cell of transmission 40%, placed in the resonator.

TABLE I

Q factors of different laser optical resonators

Optical resonator formed by:	$Q. 10^{-6}$
Mirror Z_1, flat surface of the ruby ($r_1 = 0.99$, $r_2 = 0.08$, $T = 1$.	6.85
Mirror Z_1, mirror Z_2 ($r_1 = 0.99$, $r_2 = 0.5$, $T = 1$)	12.56
Mirror Z_1, flat surface of the ruby and of the glass wall ($r_1 = 0.99$, $r_2 = 0.12$, $T = 1$)	7.13
Mirror Z_1, mirror Z_2 and kryptocyanine cell ($r_1 = 0.99$, $r_2 = 0.5$) $T = 0.075$	6.30
$T = 0.225$	6.44
$T = 0.27$	6.51
$T = 0.4$	6.82
$T = 0.5$	7.1

Nevertheless no laser spiking was observed using the first arrangement at pumping energies as high as 3500 J. On the other hand, laser operation was easily observed in the second resonator at pumping energies of some 1500 J (Fig. 7). This indicates that the Q factor of the optical cavity must be increased by bleaching of the kryptocyanine caused not by initiated laser action but by light emerging form the ruby head (from the flash tube and by fluorescence from the ruby). In the resonator formed by mirror Z_1, the flat surface of the ruby and the front wall of the glass cell, laser operation was observed irrespective of whether the cell was or was not filled with kryptocyanine. Laser operation is hardly controlled in this case because it depends on the intensity of the non-laser-light from the ruby head. When laser action is initiated between mirror Z_1 and the front wall of the cell, the laser beam bleaches the kryptocyanine and the Q factor of the optical cavity is suddenly increased. A high power light pulse of short duration might be emitted in this case. The same happens if laser action starts in the system of mirror Z_1 and the flat surface of the ruby rod. High overpumping of the laser material increases the output power of the light beam up to several or more MW. When the transmisson of the cell was some 25—30%, single laser pulses were observed at pumping energies as low as 1400 J (Fig. 8). The threshold for normal laser operation (no kryptocyanine cell in place) was 1224 J. Overpumping of the system amounts to only 14.3%. It is therefore not expected that a real giant pulse of $30 n sec$ duration could be generated in this case. Using the detecting system shown in Figs 2—5, the pulse width was measured. This pulse width determined at half power points was 1 μsec i. e. about 33 times longer that for typical giant pulse. If the concentration of the kryptocyanine was increased to obtain transmission of a few percent, the threshold for laser operation was raised up to 3260 J and no repeatable laser pulsing could be generated periodically (see Fig. 9). Laser pulses caused appreciable damage to the ruby faces, thus decreasing optical quality of the resonator. The damage exibits thread pattern and seems to be associated to strong optical inhomogeneities of the ruby crystal. It was observed that most light of the beam was emitted from a small fraction of the ruby face. The remaining part of the ruby practically did not

contribute to the generated laser beam. As seen in Fig. 9, the second and third pulses represent only 53 and 28% of the power of the first single laser pulse. Laser operation was then interrupted because of increasing damage to the ruby face. On the other hand, for kryptocyanine of relatively high transparency of 50% single laser pulses separated by few μsec can be easily generated (Fig. 10). Furthermore, laser action could be sustained with no output mirror present in the resonator. For transparency of the cell ranging from 25 to 30% single pulse operation was observed with output mirror present or even removed from the ruby resonator (pictures a, b, and c in Fig. 8). The bleaching effect was not large enough to make available the rear wall of the liquid cell for reflection of more laser light back to the resonator. Thus, laser spikes were weak and their shape diffused. Sharp single laser pulses of 1 μsec duration were generated with output mirror present in the resonator (picture d, Fig. 8).

Summarizing the experimental results the following conclusions can be drawn:

1. Kryptocyanine Q switching method enables laser spike control within wide time intervals,

2. Single pulses as well as packets of duration from several nsec up to μsec can be obtained,

3. The threshold for pumping energy in the case of single pulse operation could be lowered very close to the threshold observed for normal laser operation,

4. Bleaching of the kryptocyanine cell due to non-laser-light must be taken into account when precise laser spiking control is required.

Quite recently, Morozov and Orayevski (1967) discussed theoretically the operation conditions of a phtalocyanine Q switching passive filter and came to the conclusion that the ruby laser can generate single light pulses (half-width duration $-3\,\mu$sec) separated by 50 μsec. Similar operation conditions were obtained in this investigation using kryptocyanine passive filter.

5. High intensity laser beam within the ruby resonator

Ruby laser operating in the external mirrors optical cavity has usualy a length of 30 to 50 cm. In the experiments here presented this length was 35 cm. It consisted of almost 29 cm of light path in air ($n = 1$) and about 6 cm in ruby ($n = 1.76$). The time for passing the resonator length amounts to 1.3 nsec. This time must not be neglected with respect to the half width of a typical duration of 30 nsec of a giant laser pulse. The giant pulse is approximately triangular in shape; maximum power is thus emitted within several nsec $i. e.$ in a time interval during which the light beam can be reflected only several times by the resonator mirrors. During giant pulse operation damage to the mirrors as well as to the flat ruby faces was observed. An output mirror made of ZnS and MgF_2 multilayers evaporated on glass can be destroyed completely by a single giant laser pulse. For this reason only a hard dielectric mirror should be used as output mirror ($e. g.$ a mirror composed of a CeO_2 and MgF_2 multilayer pile). The total reflection mirror is not so critical because it does not reflect the maximum output power of the laser pulse. The most troublesome problem is the damage appearing at the polished faces of the ruby rod. This damage is not caused by the eventual existence at the surface of dust or other particles. If dust is present or if the surface is not clean enough soot spots at the surface can be found after the laser pulse. These black spots could be

easily removed by tender polishing of the ruby faces. On the other hand, damage appearing in the form of a thread pattern cannot be removed, and the ruby face has to be polished optically. In searching for the reason of the damage, the ruby faces as well as the mirrors were observed carefully and photographed during laser action. It was established that no plasma or flame appeared at these surfaces. In the case of a soft dielectric mirror as output mirror a large, burnt out spot was found after laser shot at the multilayer dielectric pile. However, no burning flame occurred at the moment. Damage to the ruby surfaces arose only during giant pulse operation of very short duration (of the order of some 30 nsec or so). When the laser was operating in a μsec régime (with kryptocyanine cell having transmission from 25 to 50%) almost no craters or other damage ensued. In these operating conditions, several hundred repeatable laser pulses could be performed. Thus, if the power of the beam does not exceed 1 MW no serious damage to the ruby faces occurs.

For an electromagnetic light wave the electric vector is parallel to the ruby faces and to the mirror layers. This renders the possibility of damage due to a field emission process improbable. Neither is there any reason for plasma to occur at these surfaces; had plasma been generated, it would have absorbed energy from the laser beam, thus reducing the Q factor of the cavity leading to interruption of laser action. The damage at the surface is a true copy of the flux density display across the beam diameter. This energy display may also be found outside the cavity using silver films on glass substrate (Kaczmarek, 1966). Craters on ruby are formed where the flux density reaches maximum values and should be associated to crystal cracking. For ruby crystal of high optical homogeneity the energy display across its diameter is more regular and the flux density does not reach "cracking" values of the crystal.

6. Propagation of laser beams in nonlinear media

Scattering of red ruby laser light by pure liquids is relatively weak and sometimes it is difficult to take a static picture of the beam propagating in a liquid cell; this is especially true for a laser giant pulse of short duration. The most sensitive films and a bright camera ($f{:}D = 1{:}1.5$) were used in these experiments. However, the laser beam could be made easily observable when propagating in a colloid solution.

Some pictures of laser beam propagation in various liquids have already been published by this author (1966). In this paper more details concerning the problem of propagation will be presented. Fig. 11 illustrates laser beam propagating in Au colloid placed in a glass cell having a length of 5 cm. The enlargement of the pictures is 3.1. The laser beam was focused by a lens $f = 10.5$ cm; the focus position is indicated in picture a) where natural light from an autocollimator is focused for comparison. The distance between the cell and laser head was approximately 50 cm; the lens was placed about 10 cm to the left with respect to the entrance glass wall of the cell. Picture b) in Fig. 11 illustrates a normal, not focused laser beam of total energy 0.3 J (duration of the pulse -400 μsec). The diameter of the most intense part of this beam was only 2.4 mm. Picture c) presents the same normal laser beam but focused by the lens. Pictures d) and e) illustrate focusing of a giant pulse beam of energies 30 and 50 mJ respectively and of duration 1 μsec. A characteristic phenomenon of

beam narrowing can be seen. The position of the focus is not visible in these pictures and the beam irrespective of the focusing process becomes narrower. The large white spots at the rear wall of the cell indicate that a fraction of the light, not visible in the cell is not propagating in the main bright beam. The smallest diameter of this main beam measured at the end of the cell was 0.51 (picture d) and 0.74 mm (picture e).

In the next series of experiments, the liquid cell was shifted by 1 cm farther with respect to the position of the lens. The new focus point is illustrated in Fig. 12 (picture a). For comparison pictures b) and c) present focusing of a normal laser beam of energy 0.57 J, taken with the camera diaphragm open and almost closed. The smallest beam diameter was 0.9 mm whem measured at the focus. Two giant pulses of energies 30 and 50 mJ, respectively, are shown in pictures d) and e). As also seen in Fig. 11, these light beams do not exibit focusing; they become narrow on passing through the cell. Carefull examination of the propagation shown in picture c) reaveled two light channels of diameter 0.2 mm each, propagating independently on the less intense and larger beam. The difference between propagation of a normal and a giant laser beam is thus very pronounced.

a) Determination of the beam shape

The beam shape was examined using thin and flat plates immersed into the liquid perpedicularly. Microscopic silver coated slide glasses or sheets of black paper were used. The beam diameter and the energy display across this diameter were made visible by evaporated material or by the burnt out craters. It is quite interesting to notice at this point that most of the immersed silver plates were completely destroyed by a single laser giant shot. Pictures a) and b) in Fig. 13 illustrate this process occuring in water. The measured flux density display over the beam diameter was very complicated and occasionally consisted of three light beams differing in intensity and in diameter between each other. Picture c) presents focusing of a giant pulse in water; the focus of the lens was placed very close to the entrance wall of the cell. A light channel of diameter 0.2 mm was formed in the focus region, but disappeared on traversing a path of some 2 cm in the liquid. Probe plates immersed in the cell did not reveal any strong light channel of small diameter at the end of the cell. The beam was almost regularly diffused.

Beam shape determinations were then performed in Au water colloid. Picture d) in Fig. 13 illustrates focusing of a normal laser beam of energy 0.5 J; divergence after passing the focus is clearly visible. This divergence was also certified using probe-plates immersed into the cell. Picture e) illustrates moreover the beam shape determination method applied to Au water colloid. In this case a giant pulse laser beam was focused. No divergence, but narrowing of the beam was observed. The length of the liquid cell was 5 cm. Pictures f) and g) illustrate more exactly the effect of focusing and narrowing of the beam in a liquid cell of 8.4 cm length for a normal (f) and a giant pulse beam (g). The beam diameters in water as well as in Au colloid were measured and the results are presented in Table II. In the case of Au water colloid two light channels were clearly visible at the probe plate as well as from the picture of the propagating beam. The channels were sourrounded by a wide cone of the remaining part of the light from the beam. As the optical path in the liquid increased the channels collapsed into one light thread having a diameter of 0.2 mm.

b) Calculation of the flux density and the electric field value for the light beam used

Total energy of the light beam was measured with a calorimeter and the pulse duration was determined from the oscilloscope display of the photodiode or photomultiplier signal.

TABLE II

Laser beam diameter *versus* the distance traversed in the liquid

Position of the probe with respect to the entrance wall of the cell in mm		4	8	10	17	27	39	42
Water	max, beam diameter	—	0.6	—	0.5	0.7	0.8	—
	diameter of the light channel	—	0.2	—	0.2	—	—	—
Au colloid	max. beam diameter	1.8	—	1.2	—	0.8	0.75	0.7
	diameter of the light channel[1]	0.8 one ch.	—	0.3 two ch.	0.3	0.3	0.2 one ch.	0.2 one ch.

[1] ch = channel.

The measured energy ranged from 10 to 100 mJ. A laser beam of such energy is capable of ionizing air and causing electric breakdown (Kaczmarek 1966). Electric breakdown of air and other gases requires a well detrmined flux density threshold. For air this threshold was found (Tomlison *et al.* 1966) to be $P = 2.10^{12}$ W/cm^2. This flux density corresponds to an electric field value of 26.8×10^6 V/cm. Let us assume a laser beam of total energy 50 mJ (duration of the pulse — 1 μsec) focused by a lens, $f = 0.4$ cm, generating electric breakdown in air. The threshold for breakdown *i. e.* for multiphoton ionization of atoms to occur can be reached in a very small volume, where the flux density is maximum. This maximum flux density can be computed from the formula

$$I_0 \cong \frac{1}{2} \frac{P}{\lambda^2 (f/D)^2}, \qquad (6.1)$$

where P denotes the total power of the beam and D—the beam diameter. In our case $f/D = 1$. We have

$$I_0 \cong \frac{1}{2} \frac{P}{\lambda^2} = 5.10^{12} \text{ W/cm}^2,$$

for total power of the beam $P = 50$ kW.

This intensity is larger than that required for breakdown (2.10^{12} W/cm^2). However, it should be noted that formula (6.1) does not account for the divergence of the laser beam; the latter could decrease the above value for maximum intensity. If lenses of longer focal length are used, the spot in the focus region is relatively large and the only way to determine its true diametr are experiments on direct measurements of the shape of the focused

beam. For a lens of $f = 0.4$ cm and a diameter of the beam $D = 4$ mm, the divergence θ increases the spot diameter at the focus to the value

$$\Delta l = f\theta.$$

Assuming $\theta = 30'$, we obtain $\Delta l = 35\ \mu$.

On the other hand, diffraction of light is relatively small in this case and causes the spot to increase to a diameter $\Delta l'$ of

$$\Delta l' = 1.22\ \frac{\lambda}{D}\ f = 0.855\ \mu.$$

In the course of these experiments a lens of $f = 10.5$ cm was normally used. Due to the beam divergence and the rather complicated structure of its shape no attempt was made to calculate the beam diameter in the focus reigon. This diameter was established experimentally using suitable probe plates immersed into the liquid cell.

Assuming the total power of the beam as 50 kW, the flux density at the focus was computed:

$$P_1 = 1.6\times10^8\ \text{W/cm}^2, \tag{6.2}$$

for a beam of diameter 0.2 mm (at the focus). In the case when the beam diameter was larger (1 mm), the flux density amounts to

$$P_2 = 1.6\times10^6\ \text{W/cm}^2. \tag{6.3}$$

Electric field strengths related to these flux densities are:

$$E_1 = 240\ \text{kV/cm, and}\ E_2 = 24\ \text{kV/cm.} \tag{6.4}$$

When the duration of the laser single pulse was shortened to 30 nsek, the respective values of the flux densities and electric field values were

$$P_1 = 0.55\times10^{10}\ \text{W/cm}^2,\ E_1 = 1.4\times10^6\ \text{V/cm, and}$$
$$P_2 = 0.53\times10^8\ \text{W/cm}^2,\ E_2 = 1.4\times10^5\ \text{V/cm.} \tag{6.5}$$

7. Contribution from electrostriction and optical orientation to propagation phenomena of laser light in liquids

a) Electrostriction

The strong electric field of the light wave causes a decrease of the liquid volume *i. e.* an increase of its density, tending to raise the refractive index and the dielectric constant measured in the optical region. Let us take a transparent dielectric medium not consisting of any kind of free electric charges. The electrostriction force per unit volume of the liquid and the respective electrostrictive pressure are given as follows (Tamm, 1949):

$$f_{es} = -\frac{1}{8\pi}\ E^2\ \nabla\varepsilon + \frac{1}{8\pi}\ \nabla\left((E^2\ \varrho\ \frac{\partial\varepsilon}{\partial\varrho} \right),$$
$$p_{el} = +\frac{1}{8\pi}\ E^2\left(\varrho\ \frac{\partial\varepsilon}{\partial\varrho} \right). \tag{7.1}$$

In the second equation the term $\nabla \varepsilon$ was neglected assuming the medium as homogeneous. E denotes the amplitude of the electric field, ϱ — the density of the liquid, and ε — the dielectric constant. The electrostrictive pressure plays an important role in the generation of supersonic vibrations of the medium associated with the well known Brillouin scattering effect. In particular, coupling between the light waves and the supersonic phonon field can lead to stimulated Brillouin scattering giving rise to sharp acoustic or to macroscopic damage of the medium. The induction vector $\vec{D}$ can be written in the following form (Fabyelinsky 1965):

$$\vec{D} = [\varepsilon + \Delta\varepsilon(p)]\,\vec{E} = \vec{E} + 4\pi(\vec{P}^L + \vec{P}^{NL}),$$

where

$$\vec{P}^L = \frac{\varepsilon - 1}{4\pi}\,\vec{E},$$

$$\vec{P}^{NL} = \frac{\Delta\varepsilon(p)}{4\pi}\,\vec{E} = \frac{1}{4\pi}\left(\varrho\,\frac{\partial\varepsilon}{\partial\varrho}\right)_s \beta_s p\vec{E}, \tag{7.2}$$

and β_s denotes the adiabatic compressibility factor. The change in dielectric constant as a function of the electrostrictive pressure is

$$\Delta\varepsilon \cong \frac{\partial\varepsilon}{\partial p}\,\Delta p = \frac{\partial\varepsilon}{\partial\varrho}\,\frac{\partial\varrho}{\partial p}\,\Delta p = \varrho\,\frac{\partial\varepsilon}{\partial\varrho}\,\beta_s\Delta p = \frac{\gamma^2\beta_s}{8\pi}\,E^2. \tag{7.3}$$

The term $\left(\varrho\,\dfrac{\partial\varepsilon}{\partial\varrho}\right) = \gamma$ is of most interest in the numerical computation procedure. In experiments, not the term $\dfrac{\partial\varepsilon}{\partial\varrho}$ but rather $\left(\varrho\,\dfrac{\partial\varepsilon}{\partial\varrho}\right)$ is usually determined. In a similar way the change in refractive index can be written as

$$\Delta n \cong \frac{\partial n}{\partial\varepsilon}\,\Delta\varepsilon = \frac{1}{2n_0}\,\Delta\varepsilon = \frac{\gamma^2\,\beta_s}{16\,\pi\,n_0}\,E^2. \tag{7.4}$$

Here, n_0 denotes the initial refractive index. We have assumed that the changes in dielectric constant and in refractive index are of an adiabatic nature; this appears to be fully reliable at high frequency optical fields. Furthermore, in the case of a giant pulse laser beam of very short duration, no appreciable heat exchange between the illuminated portion of the medium and the rest of it could take place. Changes in the dielectric constant and refractive index can be written in simple form:

$$\Delta\varepsilon = \varepsilon - \varepsilon_0 = \varepsilon_2\,E^2,$$

$$\Delta n = n - n_0 = n_2\,E^2, \tag{7.5}$$

ε_2 and n_2 are of the order of 10^{-12} in esu. We have

$$\varepsilon_2 = \frac{\gamma^2\beta_s}{8\pi,} \text{ and } n_2 = \frac{\gamma^2\,\beta_s}{16\,\pi n_0}\,.$$
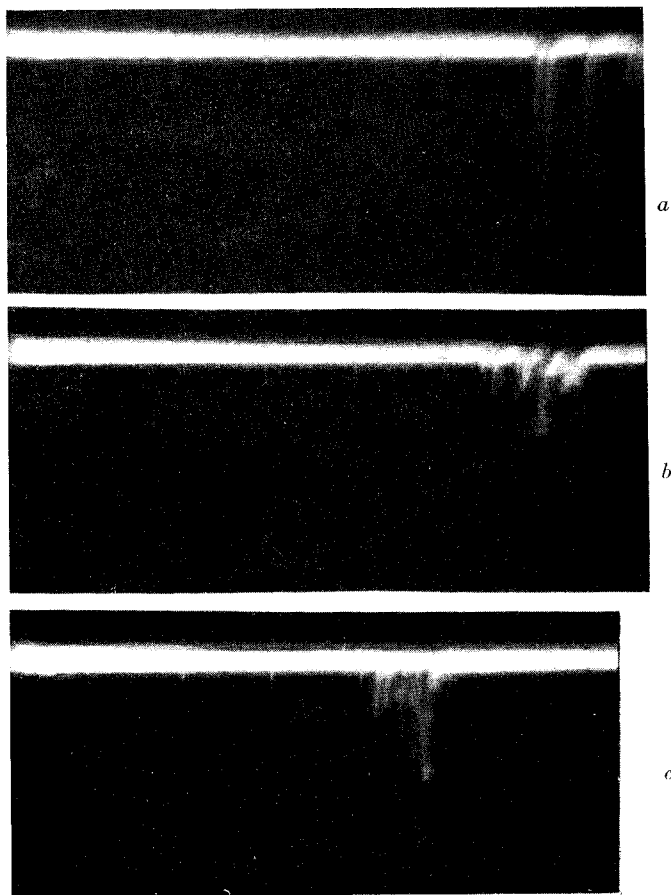
Fig. 10. Spiking of the ruby laser with a kryptocyanine Q switching cell having transmission of 50%. Time base — 50 μsec/div. a) both mirrors in place, laser spikes start after a delay i about 300 μsec, $E_p = 1975$ J, b) no output mirror in place, delay, $\tau = 275$ μsec, $E_p = 2400$ J, c) as in b), delay, $\tau = 220$ μsec, $E_p = 2960$ J
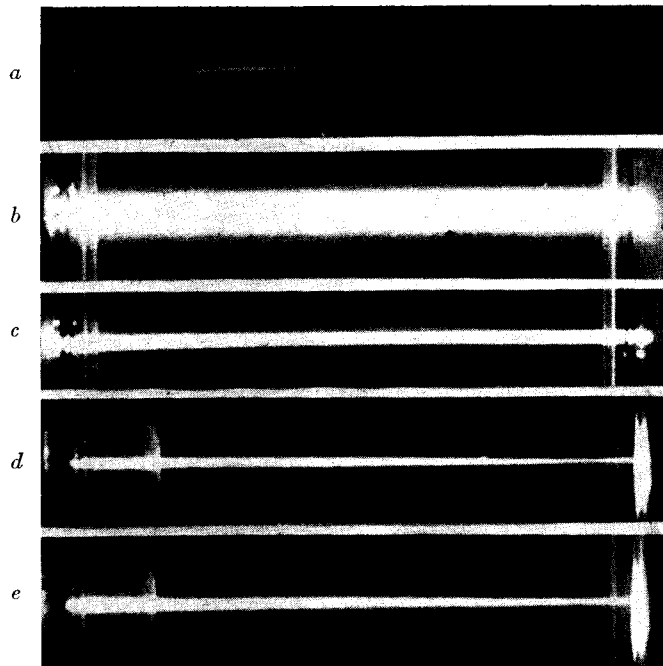
Fig. 11. Propagation of the laser beam in Au-colloid. *a*) For comparison, light from an autocollimator was focused ($f = 10.5$ cm) in the liquid cell, *b*) normal and not focused laser beam of 0.3 J energy and 400 μsec duration, *c*) normal laser beam focused, *d*) and *e*) giant laser pulses of energy 30 and 50 mJ, respectively, focused in the cell
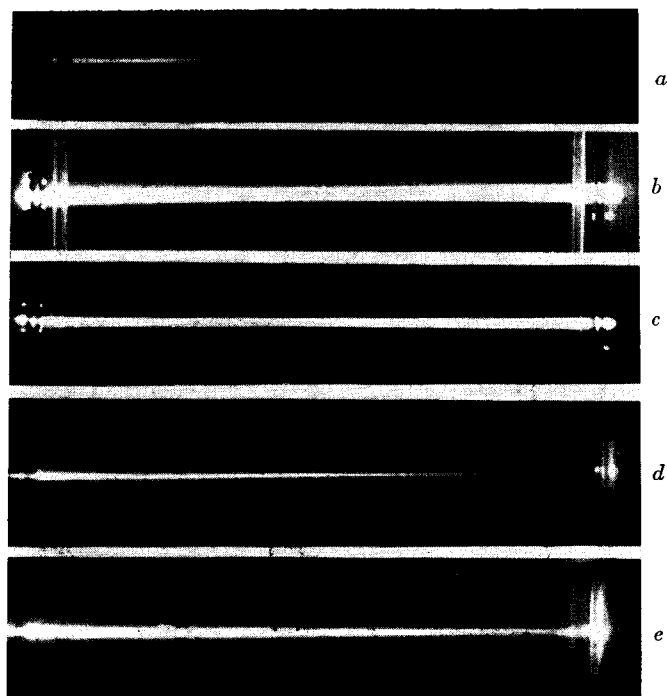
Fig. 12. As in Fig. 11 but the focus of the lens was shifted by about 1 cm to the left. Pictures *b*) an *c*) normal laser beam focused, *d*) and *e*) — giant pulse laser beam
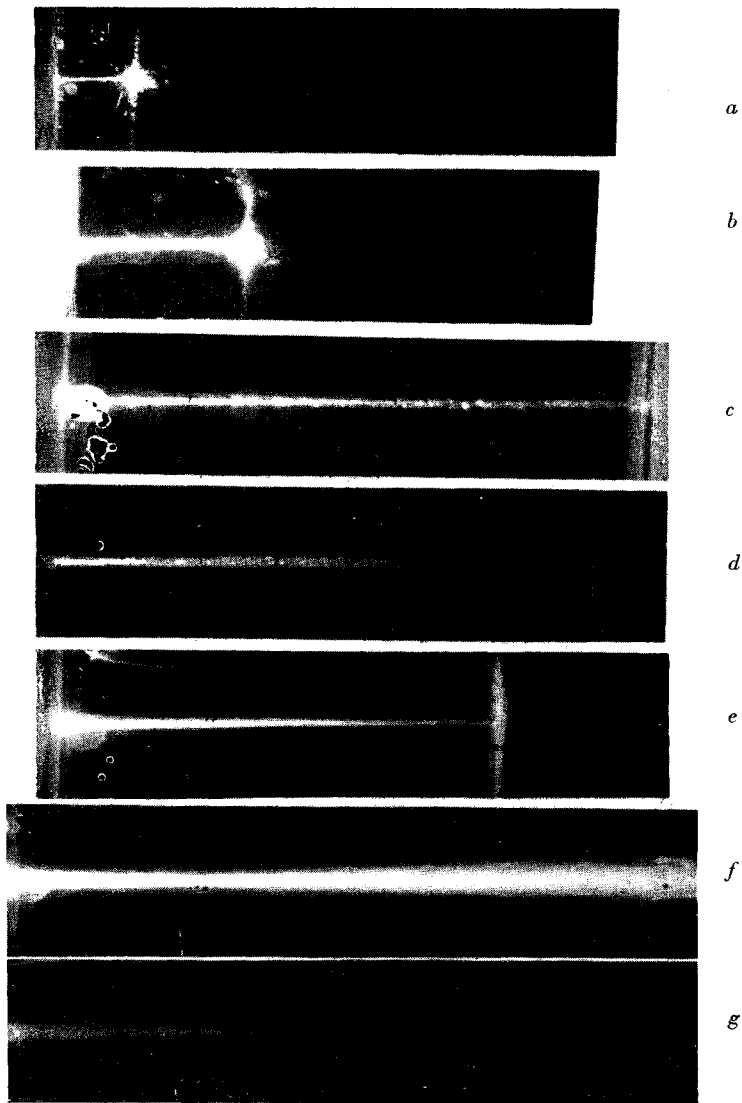
Fig. 13. Pictures illustrating determination of the laser beam shape by the method of thin plates immersed into the liquid. *a*) and *b* — giant laser pulses in water; the thin glass plate was completely destroyed by the laser shot, *c*) — water, the cell was 5 cm in length, *d*) and *f*) — normal laser beam focused in Au-colloid *e*) and *g*) — giant laser pulses in Au-colloid

Fig. 14. Illustration of plasma generated at the glass-liquid interface or at the glass-air inteface by a giant pulse ruby laser beam fairly focused by a lens, $f = 10.5$ cm, a) the cell was filled with benzene, b) — and c) — water, d) — and e) — cyklohexane, f) — nitrobenzene

If the total energy of the pulse and its duration are measured, the flux density and electric field of the wave can be computed:

$$\overline{P} = \frac{1}{2} E^2 \sqrt{\frac{\varepsilon_0}{\mu_0}} \, ,$$
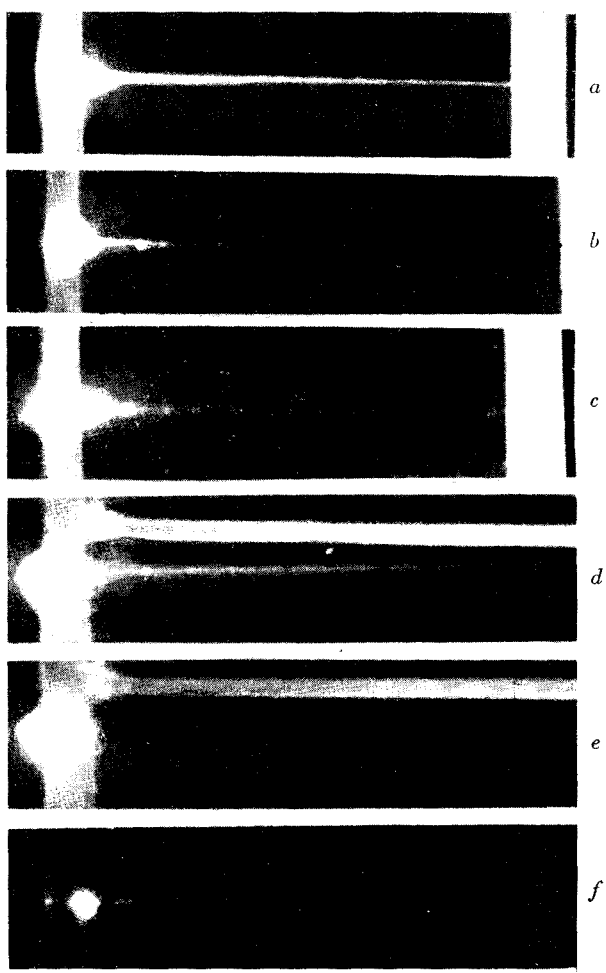
E denotes the amplitude of the field, and $\overline{P}$ — the time-averaged flux density in W/cm². If the electric field is measured in esu, it can then be inserted directly into equation (7.5) and the relation giving the changes in dielectric constant and refractive index take the form

$$\Delta\varepsilon = 8.37\times10^{-3}\, \varepsilon_2\, \overline{P},$$

$$\Delta n = 8.37\times10^{-3}\, n_2\, \overline{P}. \tag{7.6}$$

$\overline{P}$ being measured in W/cm². The quantities ε_2 and n_2 can be calculated if the term $\left(\varrho\, \dfrac{\partial\varepsilon}{\partial\varepsilon}\right)$ measured by the dynamical method is known. A first approximation consists in writing the Clausius-Mosotti equation

$$\frac{\varepsilon-1}{\varepsilon+2} = C\varrho, \qquad C = \text{const.}$$

Recurring to the dependence of ε on ϱ one can obtain a relation for $\left(\varrho\, \dfrac{\partial\varepsilon}{\partial\varrho}\right)$:

$$\varrho\, \frac{\partial\varepsilon}{\partial\varrho} = \frac{(\varepsilon+2)\,(\varepsilon-1)}{3}\, .$$

The obtained results, however, differ very much from those measured in the experiments (e. g. from the results obtained by studying scattering of light). More exact results are had from the following approximate relation (Fabyelinsky, 1965):

$$\varrho\, \frac{\partial\varepsilon}{\partial\varrho} = (\varepsilon-1),$$

in which the term $\left(\dfrac{\varepsilon+2}{3}\right)$ describing interaction between the molecule under consideration and the molecules placed outside the Lorentz sphere is omitted. If the term $\left(\varrho\, \dfrac{\partial\varepsilon}{\partial\varrho}\right)$ is experimentally determined from scattering data or from ultrasonic measurements, the most accurate results for the change in dielectric constant or in refractive index of a given liquid can be obtained. For the flux density computed above the change in refractive index due to optical electrostriction was calculated and is presented in Table III.

The numerical values of ϱ, γ, n_0 and β_s have been taken from Fabyelinsky (1965).

More details concerning the problem of the change in n as due to electrostriction were given by Shen (1966) and by Kasprowicz and Kielich (1967).

TABLE III

Change in refractive index n due to optical electrostriction

Substance	$\varrho(g/cm^3)$	γ	n_0	$\beta_s \cdot 10^{12}$	$n_2 \cdot 10^{12}$	$P(W/cm^2)$	Δn
water	0.997	0.82	1.34	45.7	0.61	$1.6.10^8$	$8.16.10^{-7}$
						$1.6.10^6$	$8.16.10^{-9}$
						$0.53.10^{10}$	$2.7.10^{-5}$
						$0.53.10^8$	$2.7.10^{-7}$
benzene	0.879	1.56	1.522	52.6	1.7	$1.6.10^8$	$2.3.10^{-6}$
						$1.6.10^6$	$2.3.10^{-8}$
						$0.53.10^{10}$	$0.76.10^{-4}$
						$0.53.10^8$	$0.76.10^{-6}$

b) Nonlinear changes in refractive index in colloid solution

In the case of a colloid solution no precise numerical values of the quantities n_0, γ and β could be found. If the laser beam exhibits selftrapping or if narrowing of the beam does appear, a certain threshold for the flux density and a given path of the beam have to be exceeded. According to Chiao et al. (1966) selftrapping can appear if, at least, the change in refractive index of the liquid compensates the diffraction loss of the beam. The critical selftrapping value of the electric field (Kelley, 1965) can be written in the form

$$E_{\text{crit}} = \frac{1.22 \lambda}{8a \, (n'_2 \, n_0)^{1/2}}, \qquad (7.8)$$

where a is the beam radius, and $n'_2 \, E^2 = \frac{n_2}{2} \, E^2$ is the nonlinear contribution to the change in refractive index:

$$n = n_0 + n'_2 \, E^2. \qquad (7.9)$$

This nonlinear contribution arises because of molecular orientation and optical electrostriction. It should be pointed out that the isotropic character of Eq. (7.9) does not mean that molecular orientation is also isotropic. As it was shown by Kielich (1966, 1967) only molecules exhibiting anisotropic optical polarizability can cause an increase or decrease in refractive index of a substance (see Eq. 8.2 of this paper). Furthermore, the beam may narrow on traversing a definite path in the substance. This characteristic distance on which the power of the beam increases pronouncedly was introduced by Kelley (1965), who estimated the following relation

$$z = \frac{a}{2} \left(\frac{n_0}{n'_2} \right)^{\frac{1}{2}} (E_{m'} - E_{\text{crit}})^{-1}, \qquad (7.10)$$

where $E_{m'}$ is the peak value of the electric field. Substituting (7.8) into (7.10) one can obtain a relation expressing the nonlinear change in refractive index n'_2 as a function of the beam

diameter, electric field value and characteristic distance z in the form

$$n_2' \cong \frac{0.305 \; \lambda z + a^3 \; n_0^{3/2} \; \sqrt{2}}{2 E_{m'} \; a \; n_0^{1/2} \; z} \; . \tag{7.11}$$

Assuming n_0 to be that of water and taking $z = 4$ cm and $a = 0.01$ cm, as normally observed, n_2' values were computed and are presented in Table IV. The relatively high increase in the refractive index of the substance should be associated to the extremely large optical anisotropy of its particles. As it can be seen, the n_2' values are by two orders in magnitude larger than those obtained for pure liquids which usually are of the order of 10^{-12} (Kielich, 1967).

TABLE IV

n_2' and Δn values calculated for Au water colloid

Beam radiu in mms	Flux density in W/cm	Peak electric field in V/cm	n_2'	Δn
0.01	1.6×10^8	2.4×10^5	1.17×10^{-10}	0.75×10^{-4}

c) Optical orientation effect

The observed changes in refractive index, especially those found in substances composed of highly anisotropic molecules, are mainly due to optical orientation. The strong electric field of the light wave induces an electric moment in the molucule which tends to rotate the latter to the position of minimum interaction energy between the electric field and this induced electric moment. The directing force is independent of the sense of the electric field. This orientation process increases the number of molecules having their maximum polarizability axes aligned with the direction of the field. This effect was first described by Buckingham (1956) and later discussed by Piekara and Kielich (1958). The optical orientation effect has been dealt with in detail in a number of papers by Kielich (1966, 1967). If the light is linearly polarized, the optically induced birefrigence can be expressed in the following way (Kielich, 1967):

$$n_{\sigma\tau}^2 - n_0^2 \, \delta_{\sigma\tau} = \left(\frac{n_0^2+2}{3}\right) \left[(3I_{\sigma\tau} - I\delta_{\sigma\tau}) \, B + AI\delta_{\sigma\tau}\right], \tag{8.2}$$

where n_0 denotes the initial refractive index, I — the intensity of the light beam, δ — Kroenecker's symbol, $n_{\sigma\tau}$ — the optical permittivity tensor, A — a constant responsible for optical deformation of the molecule. As an example, some numerical values of the induced optical anisotropy for liquids most frequently investigated computed by Kielich (1967) are presented in Table V.

As seen from Table V and III, the contributions from optical orientation and electrostriction to the change in refractive index are of the same order in the case of molecules of low optical

TABLE V

Change in refractive index due to optical orientation of the molecules

substance	$\Delta n = n_{||} - n_{\perp}$
water	$(3.29-5.50) \cdot 10^{-12}$
benzene	$(0.08-0.1) \cdot 10^{-12}$

anisotropy. The effect of electrostriction does not depend on the optical anisotropy; this means that when the refractive index of the liquid under investigation achieves very high values it must be associated solely to the optical orientation process.

d) Electrostriction pressure in illuminated liquids

A liquid illuminated by an intense laser beam undergoes changes in density which generate macroscopic motion in some fraction of the liquid. This increase in pressure could be calculated using formula (7.1)

$$\Delta p = \frac{1}{8\pi} E^2 \left(\varrho \frac{\partial \varepsilon}{\partial \varrho} \right).$$

Here Δp is measured in dyne/cm², and E — in esu. In the course of these experiments flux densities of the order of 10 MW/cm² in the focus region of the liquid were easily obtained. Computation of the pressure increase for this flux density gave the following numerical results:

water, $\Delta p = 0.0028$ Atm; benzene, $\Delta p = 0.0053$ Atm.

The change in pressure generates elastic waves inside the liquid. Pictures of highly disturbed propagation, as is believed, partially due to such elastic waves were shown by this author (1966). The static pictures exhibited shock waves arising during the laser pulse as well as in the time interval of about 1 sec after the pulse had ceased. Using a lens of $f = 5$ cm, the beam diameter was reduced in the focus region to less than 0.1 mm. In some laser shots a flux density of 500 MW/cm² was reached in the focus of this lens. The pressure increase was higher in this case and had the following value:

water, $\Delta p = 0.14$ Atm; benzene, $\Delta p = 0.255$ Atm.

These values are large enough to cause observable disturbance of the liquid illuminated by the laser beam. In the case of transparent liquid media no serious heating effects occured. The amount of energy absorbed by the liquid from the laser beam was measured using an appropriate calorimeter, and appears to be very small. A giant pulse laser beam of energy of the order of 100 mJ is thus not able to raise the temperature of the liquid.

8. Generation of plasma in a giant pulse laser beam

a) Experimental results

At high power level of the laser beam, when the latter is focused in the liquid, plasma generated at the glass-liquid interface or within the liquid was observed. Experimental

results concerning this problem were described by this author earlier (1966) and recently by Dowley *et. al.* (1967). Some new results on plasma generated at the interface are presented in this paper. The most striking effect was found in benzene (picture *e* in Fig. 14). Strong plasma generated at the glass-liquid interface caused damage to the wall in the form of a circular crater having a diameter of some 1.5 mm. The laser beam was fairly focused at the cell using a lens, $f = 10.5$ cm. Previous to the second successive laser shot, the benzene was removed from the cell. No plasma at the glass wall was visible in this case (the power of the beam was kept at a constant level). Thus, threshold for breakdown is lowered by the presence of the liquid. Pictures *b*) and *c*) illustrate plasma generated in water, *d*) and *e*) in cyclohexane, and *f*) — in nitrobenzene. As it can be seen, plasma in some cases appears to be stronger at the interface, and in other cases at the front wall of the cell. Nevertheless, lowest threshold for breakdown, irrespective of the kind of the liquid, was observed at the glass liquid interface but not at the front wall of the cell. Plasma absorbs most of the radiation energy from the laser beam and tends to grow in the direction of the laser device. Attenuation of the laser beam by the generated plasma can be seen in picture *e*) (Fig. 14). Breakdown initiated at the glass-liquid interface very often moves towards the front side of the wall, where it starts to grow in intensity (*e. g.* pictures *d*) and *f*) in Fig. 14). The breakdown is always associated with blue-violet luminescence and a short acoustic burst. Occasionally ionization in the laser beam path of the liquid was observed in the form of a line of dashed blue-violet strips. Careful examination of this process indicates that ionization was initiated at small impurity centers present in the liquid.

b) Discussion of the problem of optical beakdown of dense media

Breakdown of air and other gases and plasma generated at solid surfaces were investigated by many authors (Archbold 1964, Bernal *et .al.* 1965, Basov *et. al.* 1967, Rayzer 1965). However, as yet little work had been devoted to the study of generation of plasma at a solid-liquid interface or within liquid substances. The observations described recently by Dowley and co-workers (1967) are in good agreement with those previously described by this author (1966) and with the results presented in this paper.

In general, photoionization of an atom may occur if the incident light quantum represents energy comparable to the ionization energy of this atom. In the case of the ruby laser beam, the energy of the light quantum is only 1.78 eV, *i. e.* almost ten times smaller that the ionization energy of a noble gas atom. Consider now a solid or liquid target made of conducting material. The work function for an electron to be withdrawn from the surface is, on the average, several times larger than the above value of 1.78 eV. Thus, ionization leading to generation of a strong plasma is caused by an avalanche process which is initiated by free electrons released from adsorbed and surface atoms by photoionization in the laser beam and by thermoemission from the surface. It should be pointed out that the thermoemission process may not contribute to generation of the plasma. Furthermore, strong emission of ions and electrons by laser beam irradiated metallic surfaces is not necessarily associated with generation of visible plasma.

Let us now consider electric breakdown caused by an oscillating field. If the oscillation frequency is high enough, it can happen that the accelerated electron has no chance to trans-

fer its energy (in a half period time interval) to neutral atoms or molecules because of lack of collisions. Thus, the mean free path length plays an important role in the process of high frequency electric breakdown. In the case of a gaseous substance this free path length can be easily changed by varying the pressure. Thus, the free path length in air ($p = 1$ Atm, $T = 0°C$) is of the order of 10^{-6} cm, and can be decreased to several Å when the pressure is raised to about 100 Atm. As known (Minck, 1944), gaseous substances under a pressure of some 100 Atm break down at a flux density threshold similar to that characteristic for dense isotropic media. From the point of view of electric breakdown non-crystalline solids and liquids may be treated as compressed gases. In a dense substance the free path length is so small that the oscillating electron (in the electric field of the light wave) is retarded in the collision process and energy from the light beam can be transfered to neutral atoms. The latter could be excited or ionized.

The threshold for breakdown at the glass-liquid interface is relatively low, meaning that free electrons are easily generated there. These free electrons initiate an avalanche process which causes the plasma to grow in intensity. Let us now consider the status of the interface in detail. Firstly, it can be covered by adsorbed impurity atoms or ions. A neutral atom can be adsorbed as an ion, while the free electron is captured by the surface. The interface can adsorb atoms or ions depending on the relation between the ionization energy I of the atom, work function Φ of the surface, and potential energy E at the interface. Neutral atoms can be adsorbed by the solid surface in the form of positive ions if (Dekker 1960)

$$E_j - (I - \Phi) > E_a$$

On the other hand, atoms may become adsorbed without ionization if

$$E_j - (I - \Phi) < E_a.$$

Thus, atoms having low ionization energy may be adsorbed by the glass wall as positive ions. In fact, numerous observations of strong positive ion emission from various surfaces illuminated by a giant pulse laser beam are known (Bernal 1966, Perressuni 1966, Ducauze 1965, Archbold 1965). It is very interesting to point out that even in the case of very clean surfaces, various impurity ions adsorbed thereon were emitted (e. g. a tungsten surface emitted Na^+, K^+, Ca^+, H^+, H_2O^+ and other ions). The amount of surface material ions emitted was found to be only some 20% of the total amount of the emitted ions.

Positive ions adsorbed by the surface do not decrease the threshold for breakdown because its ionization requires higher energies than those for neutral atoms. However, the free electrons forming an electric double layer at the interface with the positive ions may contribute to some extent towards initiation of ionization. Furthermore, the presence of the double layer decreases the work function of the solid surface. Table VI presents some numerical values of refractive indices, dielectric permittivities, ionization energies, and work functions for the relevant substances or ions. As seen, liquids in which plasma was observed represent almost the same ionization energies. Neither are there considerable differences in the refractive index values or dielectric permittivities.

For this reason, slight variations in the threshold values of these liquids should rather be associated to the amount of different impurities present therein and not to specific properties of the molecules. In the case of a glass wall, ionization of alkali atoms adsorbed by the surface

TABLE VI

Substance	Refr. index n			Diel. perm. $\varepsilon = n^2$			Ioniz. energy I (eV)	
water	1.389			1.79			12.59	
benzene	1.522			2.32			9.245	
nitrobenzene	1.66			2.425			—	
cyclohexane	1.426			2.05			9.08	
n-hexane	1.38			1.9			10.017	
carbon disulphide	1.673			2.8			10.02	

atom or molecule	Li	Na	K	Ca	Ba	BaO	H_2O	SiO_2
work function Φ in eV	5.39	5.138	4.339	6.111	5.81	1.0—1.6	6.1	5.0

and of different oxides of very small work functions (see Table VI) could be initiated at a flux density of the lihgt beam several times lower that in the case of gaseous substance. Once the ionization process is initiated it can develop into an avalanche process because of the small free path length in the dense medium, and because of the relatively large diffusion coefficient. Plasma begins to grow rapidly in intensity if the number of electrons released in the multiphotoionization process and in other processes exceeds the number of electrons diffusing from the breakdown region to the neutral environment. The diffusion coefficient for electrons which appears in the equation describing diffusion-like mechanism of electric breakdown (*e. g.* Skanavi 1958) is much larger than in the case of a gaseous substance. Thus, the avalanche process can be easily sustained or increased in the focus volume of a dense medium.

Damage to the glass wall of the cell is caused by the plasma which moves in the direction of the front wall. On the other hand, if the plasma is solely initiated at the front wall of the cell (at higher flux densities) it tends to escape from the wall and as a result of this process, practically no damage is caused to the surface. It should be kept in mind that plasma generation is an explosive process (Basov *et al.* 1966) and almost all the energy on the laser beam is transferred to the plasma within a time interval of 1 μsec or several nsec.

REFERENCES

Archbold, E., Harper, B. W., Hughes, T. P., *Brit. J. Appl. Phys.*, **15**, 1321 (1964).
Baker, R. M., *Electronics*, **1**, 36 (1963).
Basov, N. G., Boyko, V. A., Demyenthyev, V. A., Krokhin, O. N., Sklyshkov, G. V., *Zh. Exper. Teor. Fiz.*, **51**, 989 (1966).

Basov. N. G., Boyko, V. A., Voynov, Y. P., Kononov, E. Y., Mandelshtam, C. L., Sklyshkov, G. V., *Pisma v Redakt.*, **5,** 177 (1967).

Bernal, E., Ready, J. F., *Phys. Letters*, **19,** 645 (1966).

Buckingham, A. D., *Proc. Phys. Soc.*, *B69*, 344 (1956).

Chiao, R. Y., Garmire, E., Townes, C. H., *Phys. Rev. Letters*, **13,** 479 (1966).

Chiao, R. Y., Garmire, E., Townes, C. H., *Phys. Rev. Letters*, **16,** 347 (1966).

Dekker, A. J., *Solid State Physics*, Ed. Prentice-Hall Inc., 1960.

Dowley, M. W., Eisenthal, K. B., Peticolas, W. L., *Phys. Rev. Letters*, **18,** 531 (1967).

Ducauze, A., Tonon, G., Veyrie, P., *C. R. Acad. Sci. Paris*, **261,** 4039 (1965).

Fabyelinskiy, E. J., *Molekularnoye Rasseyanye Svyeta*, Ed. Nauka, Moskva 1949.

Goodwin, D. W., *ZAMP*, **16,** 35 (1965).

Granovskiy, W. L., *Elektricheskyi Tok v Gazakh*, vol. I, Moskva 1952.

Kaczmarek, F., *Acta Phys. Polon.*, **30,** 877 (1966).

Kaczmarek, F., *Acta Phys. Polon.*, **30,** 891 (1966).

Kaczmarek, F., Graja, A., Drobnik, A., Planner, A., *Fiz. Diel. i Radiospektroskopia*, **4,** (1967), Poznań, in print.

Kasprowicz, B., Kielich, S., *Acta Phys. Polon.*, **31,** 787 (1967).

Kelley, P. L., *Phys. Rev. Letters*, **15,** 1005 (1965).

Kielich, S., *Acta Phys. Polon.*, **30,** 683 (1966).

Kielich, S., *Acta Phys. Polon.*, **31,** 689 (1967).

Kielich, S., *Proc. Phys. Soc.*, **90,** 847 (1967).

Kielich, S., *Phys. Letters*, **24***A*, 383 (1967).

Minck, R. W., *J. Appl. Phys.*, **35,** 252 (1964).

Morozov, W. N., Orayevski, A. N., *Zh. Exper. Teor. Fiz.*, **37,** 947 (1967).

Peressini, E. R., *Physics of Quantum Electronics*, p. 499 (1966). Ed. Kelly, P. L., Lax, B., Tannenwald, P. E., McGraw-Hill.

Piekara, A., Kielich, S., *Archives des Sciences*, 11, Fasc. Spec., 1958,

Piekara, A., Kielich, S., *III Conf. on Quantum Electronics*, Paris, **2,** 1062 (1962).

Rayzer, U. P., *Uspekh. Fiz. Nauk.*, **87,** 29 (1965).

Shen, R. Y., *Phys. Letters*, **20,** 378 (1966).

Skanavi, G. I., *Fizika Dielektrikov*, Moskva 1958.

Tamm, I. E., *Kurs Teoryi Elektrichestva*, Moskva 1949.

Tomlison, R. G., Daman, E. K., Buscher, H. T., *Physics of Quantum Electronics*, p. 520, 1966.